The American Journal of Human Genetics, Volume *105*

Supplemental Data

Bi-allelic Variants in *METTL5* Cause Autosomal-Recessive Intellectual Disability and Microcephaly

Elodie M. Richard, Daniel L. Polla, Muhammad Zaman Assir, Minerva Contreras, Mohsin Shahzad, Asma A. Khan, Attia Razzaq, Javed Akram, Moazzam N. Tarar, Thomas A. Blanpied, Zubair M. Ahmed, Rami Abou Jamra, Dagmar Wieczorek, Hans van Bokhoven, Sheikh Riazuddin, and Saima Riazuddin

Supplemental note:

Case reports

For family PKMR43M, both parents of affected individuals have been interviewed to obtain information on prenatal, perinatal, and neonatal medical history and developmental milestones. A detailed history of neurological and systemic symptoms was obtained and functional capacity including self-care, education, special needs and social interaction was documented. Physical examination of all affected and unaffected children included documenting of motor milestones, weight, height, head circumference, morphological abnormality screening, musculoskeletal features, deep tendon reflexes, gait, cerebellar functions, and verbal and motor aptitude. Furthermore, all affected individuals have been clinically evaluated for any ophthalmological, audiological, vestibular, or dermatological abnormalities. ID severity has been classified as severe based on measures of developmental milestones /criteria from American Association on Intellectual & Developmental Disability.

In addition to phenotypic features presented in the main text, all three affected individuals of PKMR43 had considerable delay (months to years) in childhood development milestones in all domains including cognitive development, social and emotional development, speech and language development, and gross motor and fine motor skill development. At the time of evaluation, all three individuals could understand speech but were unable to communicate. They could eat and drink but needed significant supervision for execution of other activities of daily living. All individuals had aggressive behavior. They could not travel alone. Brain MRI were acquired after the first evaluation of the family, based on the microcephaly of the affected individuals.

For family F47949, we had interviews with the parents and physical examinations of the brothers in our department as described above. No formal IQ testing was performed. ID severity has been classified as severe based on criteria described in Zhang et al [1]. Patient III:2 has an IQ between 20 and 35 (moderate to severe) and patient III:3 has an IQ between 10 and 20 (severe). The elder brothers learned walking without support at the age of 3 years and was able to talk simple sentences at the age of 9 years. He was not able to write, read or calculate. The younger brother learned walking at the age of 3,5 years, he did not speak any word at the age of nearly 5 years. Both brothers were biting their hands.

For family from Hu et al (2019), HAWIK-IV showed IQs of 25 and 26 for patients III:3 and III:5, respectively [2].

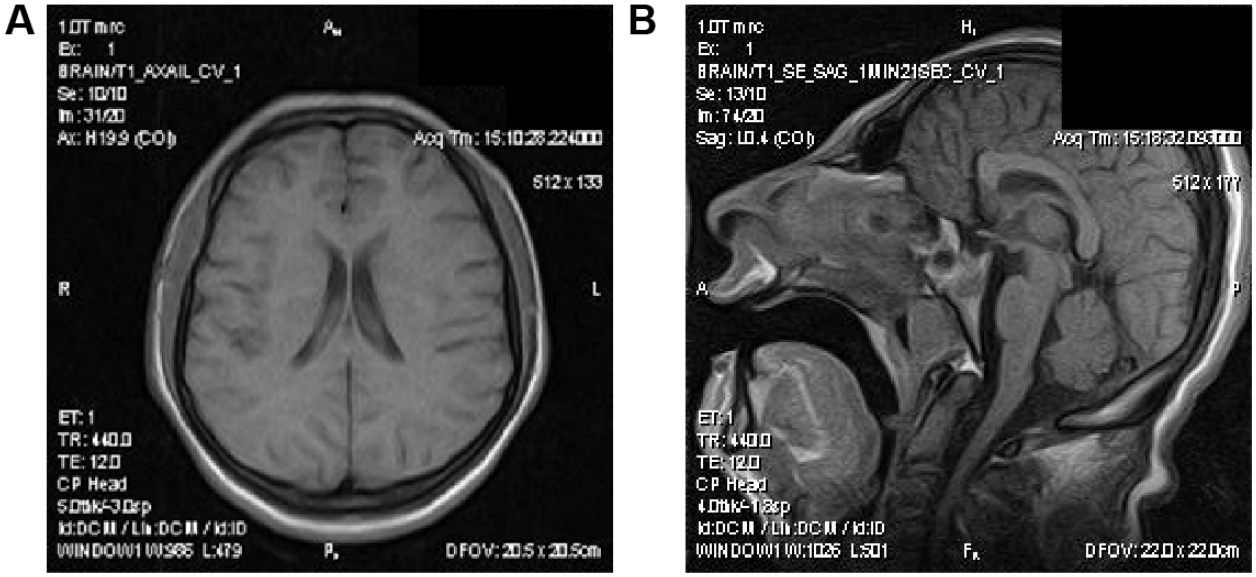

Figure S1. MRI of individual PKMR43M II-2 confirms microcephaly.

(A) MRI of an axial section of individual PKMR43M II-2 brain while (B) MRI of a sagittal section confirms microcephaly.

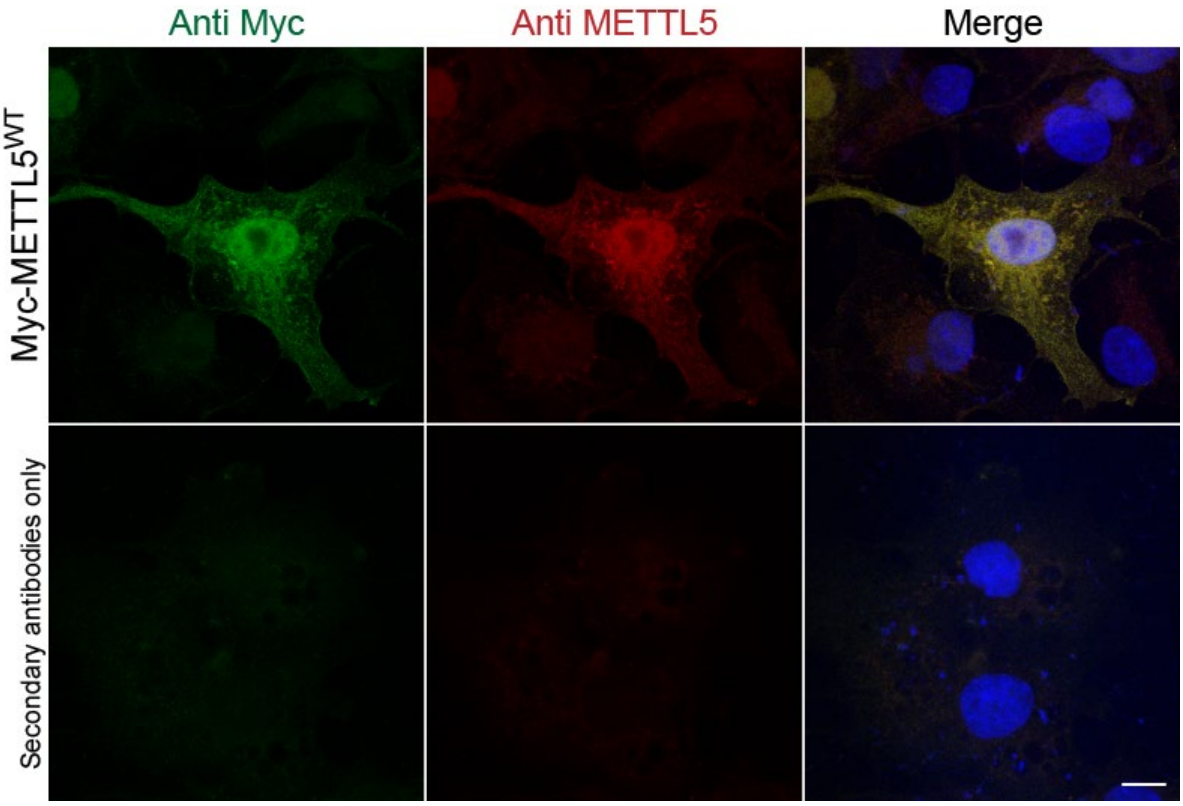

Figure S2. Validation of METTL5 (Novus Biologicals) antibody.

To validate the METTL5 antibody, COS7 cells were transiently transfected with Myc-METTL5 cDNA construct. After 48h, the cells were fixed, permeabilized and immunolabeled with a Myc antibody (Covance Research Products Inc Cat# MMS-164P-100, RRID:AB_291335) and METTL5 antibody (Novus Biologicals Cat# NBP1-56640, RRID:AB_11039697). The nuclei were counterstained with DAPI (blue). Myc staining (green) and METTL5 staining (red) colocalize (merge) showing that METTL5 antibody can recognize the transfected protein. The bottom panel represent cells that were submitted to the same immunolabeling protocol with the exception of the incubation with the primary antibodies, namely Myc and METTL5. No signal was detected in this specific case. All images are projection of confocal optical sections stack. Scale bar: 10µm.

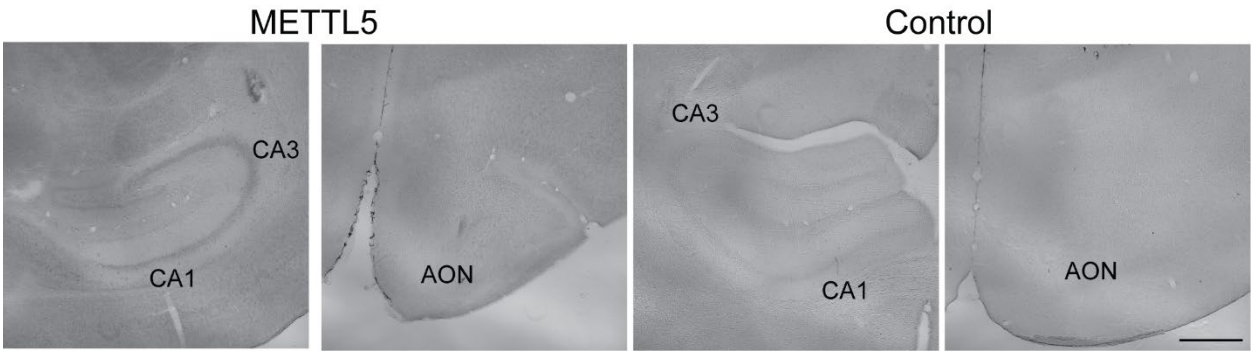

Figure S3. Immunolocalization of Mettl5 in the mouse brain.

Immunolocalization of Mettl5 in P30 mouse brain, using a 3,3′-Diaminobenzidine (DAB) based immunochemistry procedure, shows a faint and diffuse staining in different structures, absent in the control slices (no primary antibody). CA1 and CA3 of the hippocampus, AON: anterior olfactory nucleus. Scale bar: 500μm.

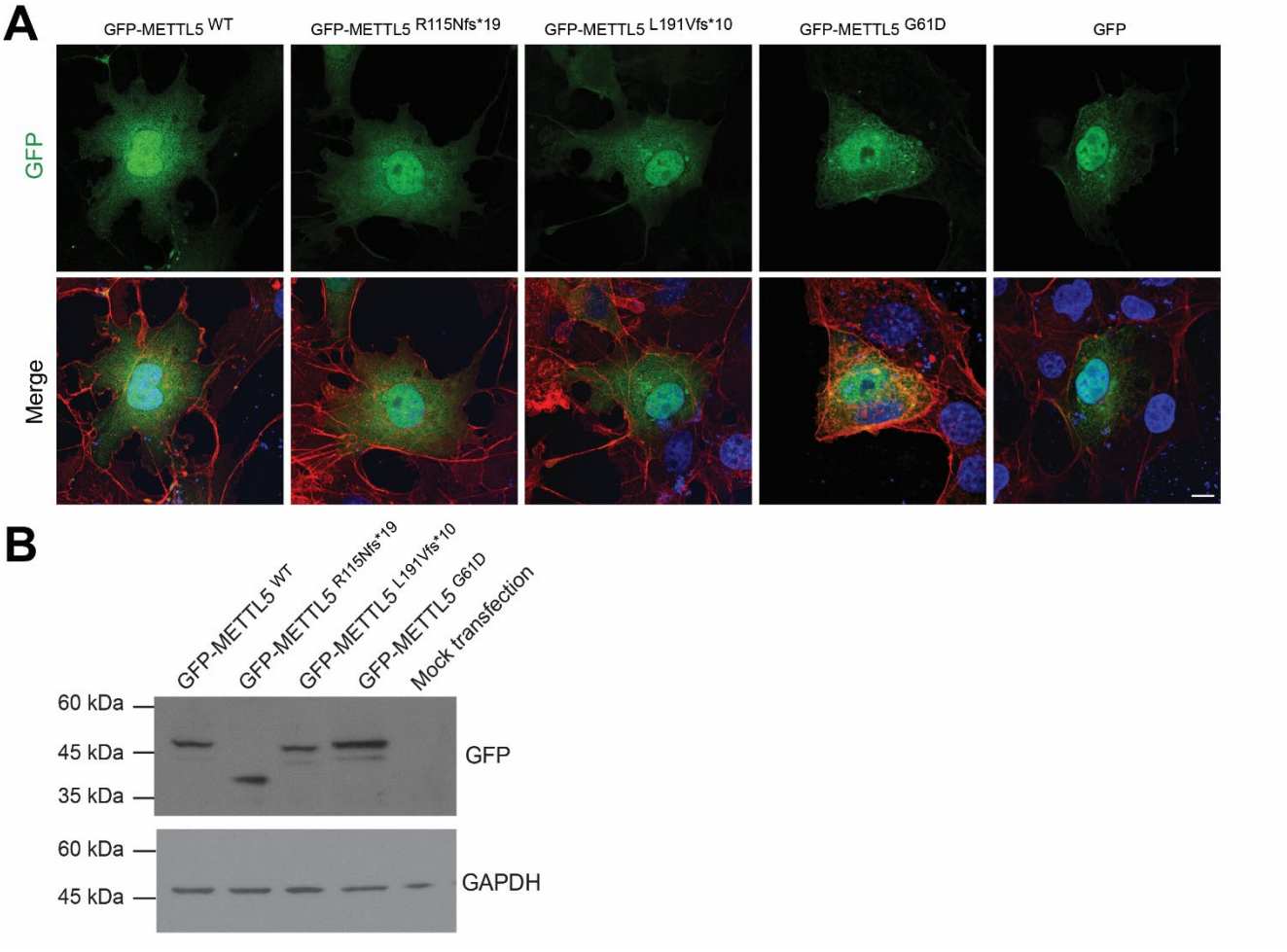

Figure S4. Steady state level and localization of GFP-METTL5.

To validate the results obtained with Myc-METTL5, we performed localization in transfected COS7 cells and Western Blot analysis on transfected HEK cells with GFP-METTL5 constructs. (A) GFP-METTL5 fusion proteins for WT and the 3 variants associated with ID, after transfection in COS7 cells. The subcellular localization shows that, like Myc-METTL5 proteins, GFP-METTL5 WT and the three disease-associated mutant proteins (green) accumulate in the nucleus (blue) and forms aggregates in the cytoplasm. All images are projection of confocal optical sections stack. Scale bar: 10µm. (B) Western Blot on transfected HEK293T cells with GFP-METTL5 WT or mutant constructs, using GFP antibodies (Molecular Probes Cat# A-11122, RRID:AB_221569) did not reveal any decrease of the steady state level of the mutant proteins. We hypothesized that the GFP tag, due to its large size (27kDa), is conferring stability to the synthesized mutant proteins METTL5 ^{R115Nfs*19} and METTL5^{L191Vfs*10} (15kDa and 23kDa respectively). GAPDH (Santa Cruz Biotechnology Cat# sc-32233, RRID:AB_627679) was used as loading control.

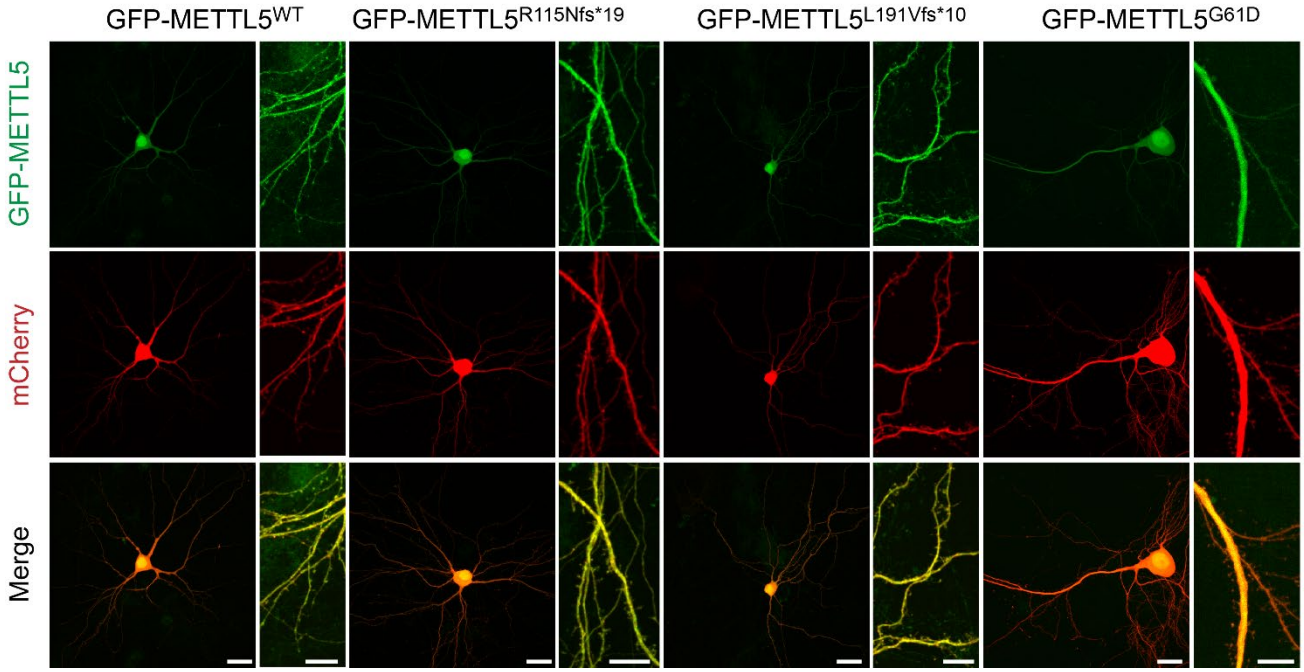

Figure S5. METTL5 variants do not affect the synapse morphology.

Transfected rat hippocampal neurons with GFP-METTL5 fusion proteins for WT and the three disease-causing variants (green) constructs and pmCherry-N1 vector (Takara, red). None of the variant affect the morphology of the dendrites nor localization of the protein in transfected neurons. All images are projection of confocal optical sections stack. Scale bars: 24 and 10μm.

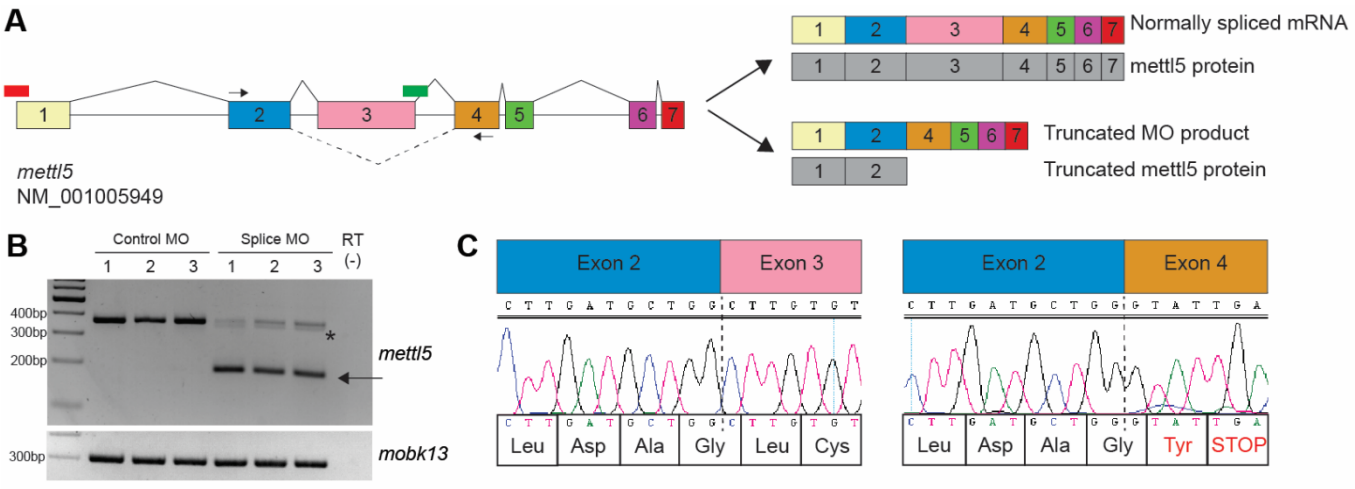

Figure S6. Anti-sense *mettl5* morpholino retains intron 4 and leads to a truncated protein. (A) Schematic diagram of the zebrafish *mettl5* gene, showing: exons (numbered blocks); ATG MO and splice MO targets (red and green blocks, respectively); PCR primers flanking exon 3 (black arrows, sequences are available upon request). (B) Knockdown in splice-targeting MO injected embryos was verified using RT-PCR. Embryos were injected with a Control MO (5ng) or *mettl5* splice-targeting MO (5ng). Arrow indicates the alternative splice products induced by *mettl5* splice-targeting MO injection. An additional band, indicated by an asterisk (*), was produced due to the activation of a cryptic splice site in exon 3. (C) Sanger sequencing of PCR products confirmed that injection of *mettl5* splice-targeting MO results in the absence of exon 3. A novel, in-frame, pre-mature stop codon was generated in exon 4.

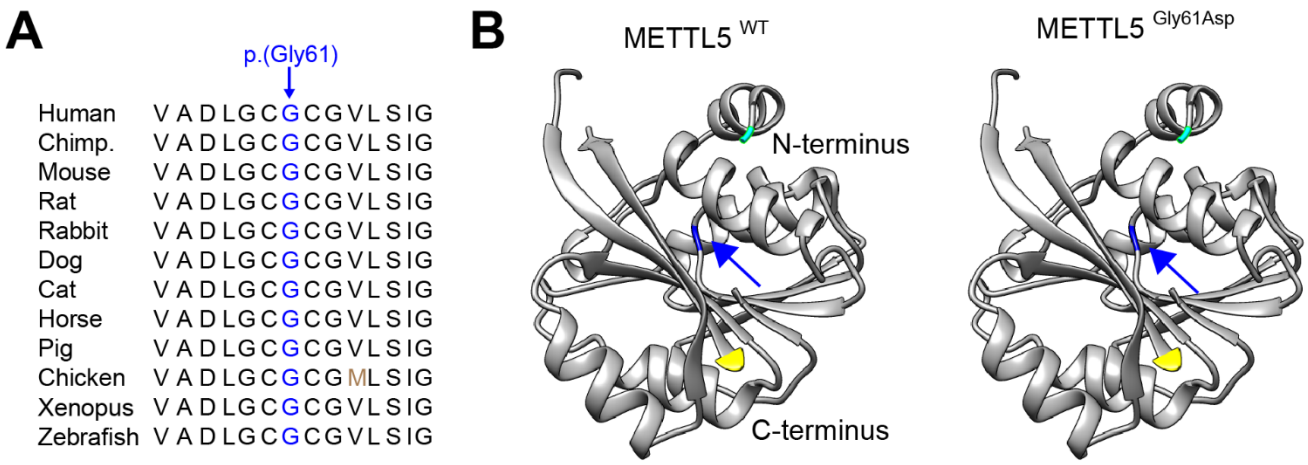

Figure S7. METTL5 p.(G61) is highly conserved among species but p.(G61D) variant does not affect the conformation of the mutant protein.
(A) The glycine residue at amino-acid position 61, depicted in blue, is completely conserved across a wide variety of species. (B) Protein modeling of the WT and METTL5^{G61D} proteins, using PHYRE2 software [3] shows that the overall conformation of the protein is not affected.

Table S2: Classification of the candidate variants based on ACMG guidelines

	Classification	**ACMG criteria used [4]**
c.182G>A; p.(Gly61Asp)	Variant of uncertain significance	PM2, PP1, PP3
c.344_345delGA; p.(Arg115Asnfs*19)	Pathogenic	PS3, PM2, PM4, PP1, PP3
c.571_572delAA; p.(Lys191Valfs*10)	Pathogenic	PS3, PM2, PM4, PP1, PP3

Table S3: Pathogenicity prediction results for *METTL5* variant [c.182G>A; p.(Gly61Asp)]

c.DNA variant	Protein variant	Polyphen-2(1)		PROVEAN (2) (score)	SIFT (3) (score)	Mutation Taster(4) (score)	gnomAD(5) frequency	ExAC(6) frequency	CADD(7) score
		HUM-DIV (score)	HUM-VAR (score)						
c.182G>A	p.(Gly61Asp)	Probably damaging (1)	Probably damaging (1)	Deleterious (-7)	Damaging (0)	Disease causing (0.999)	NA	NA	26

(1) Polyphen-2, http://genetics.bwh.harvard.edu/pph2, cut-off: <0.15 (possibly damaging) [5]
(2) PROVEAN, http://provean.jcvi.org/genome_submit_2.php?species=human, cut-off: <-2.5 (damaging) [6; 7]
(3) SIFT (from PROVEAN), http://provean.jcvi.org/genome_submit_2.php?species=human, cut-off: <0.05 (damaging) [8]
(4) MutationTaster, http://www.mutationtaster.org/, cut-off: 1 = high confidence of prediction
(5) gnomAD, genome Aggregation Database, https://gnomad.broadinstitute.org [9]
(6) ExAC, Exome Aggregation Consortium , http://exac.broadinstitute.org [9]
(7) CADD, Combined Annotation Dependent Depletion, https://cadd.gs.washington.edu [10; 11]

Supplemental References

1. Zhang, X., Snijders, A., Segraves, R., Zhang, X., Niebuhr, A., Albertson, D., Yang, H., Gray, J., Niebuhr, E., Bolund, L., et al. (2005). High-resolution mapping of genotype-phenotype relationships in cri du chat syndrome using array comparative genomic hybridization. Am J Hum Genet 76, 312-326.
2. Hu, H., Kahrizi, K., Musante, L., Fattahi, Z., Herwig, R., Hosseini, M., Oppitz, C., Abedini, S.S., Suckow, V., Larti, F., et al. (2018). Genetics of intellectual disability in consanguineous families. Mol Psychiatry 24, 1027-1039.
3. Kelley, L.A., Mezulis, S., Yates, C.M., Wass, M.N., and Sternberg, M.J. (2015). The Phyre2 web portal for protein modeling, prediction and analysis. Nat Protoc 10, 845-858.
4. Richards, S., Aziz, N., Bale, S., Bick, D., Das, S., Gastier-Foster, J., Grody, W.W., Hegde, M., Lyon, E., Spector, E., et al. (2015). Standards and guidelines for the interpretation of sequence variants: a joint consensus recommendation of the American College of Medical Genetics and Genomics and the Association for Molecular Pathology. Genet Med 17, 405-424.
5. Adzhubei, I., Jordan, D.M., and Sunyaev, S.R. (2013). Predicting functional effect of human missense mutations using PolyPhen-2. Curr Protoc Hum Genet Chapter 7, Unit7 20.
6. Choi, Y., Sims, G.E., Murphy, S., Miller, J.R., and Chan, A.P. (2012). Predicting the functional effect of amino acid substitutions and indels. PLoS One 7, e46688.
7. Choi, Y., and Chan, A.P. (2015). PROVEAN web server: a tool to predict the functional effect of amino acid substitutions and indels. Bioinformatics 31, 2745-2747.
8. Sim, N.L., Kumar, P., Hu, J., Henikoff, S., Schneider, G., and Ng, P.C. (2012). SIFT web server: predicting effects of amino acid substitutions on proteins. Nucleic Acids Res 40, W452-457.
9. Lek, M., Karczewski, K.J., Minikel, E.V., Samocha, K.E., Banks, E., Fennell, T., O'Donnell-Luria, A.H., Ware, J.S., Hill, A.J., Cummings, B.B., et al. (2016). Analysis of protein-coding genetic variation in 60,706 humans. Nature 536, 285-291.
10. Kircher, M., Witten, D.M., Jain, P., O'Roak, B.J., Cooper, G.M., and Shendure, J. (2014). A general framework for estimating the relative pathogenicity of human genetic variants. Nat Genet 46, 310-315.
11. Rentzsch, P., Witten, D., Cooper, G.M., Shendure, J., and Kircher, M. (2019). CADD: predicting the deleteriousness of variants throughout the human genome. Nucleic Acids Res 47, D886-D894.